



Photocatalytic degradation of 2,4,6-trichlorophenol in aqueous solutions using synthesized Fe-doped TiO₂ nanoparticles via response surface methodology

Anis Jahantiq^a, Reza Ghanbari^b, Ayat Hossein Panahi^c, Seyed Davoud Ashrafi^d,
Aram Dokht Khatibi^a, Elham Noorabadi^a, Ali Meshkinian^a, Hossein Kamani^{a,*}

^aHealth Promotion Research Center, Zahedan University of Medical Sciences, Zahedan, Iran, Tel. +989155412919; Fax: +985433295837; emails: hossein_kamani@yahoo.com (H. Kamani), a.jahantiq1015@gmail.com (A. Jahantiq), khatibi.aram@gmail.com (A.D. Khatibi), noorabadi.elham@yahoo.com (E. Noorabadi), meshkinian@hotmail.com (A. Meshkinian)

^bSocial Determinants of Health Research Center, Qazvin University of Medical Sciences, Qazvin, Iran, email: ghanbari33@gmail.com (R. Ghanbari)

^cSocial Determinants of Health Research Center, Birjand University of Medical Sciences, Birjand, Iran, email: ayatpanahi@yahoo.com (A.H. Panahi)

^dDepartment of Environmental Health Engineering, Research Center of Health and Environment, School of Health, Guilan University of Medical Sciences, Rasht, Iran email: d_ashrafi@yahoo.com (S.D. Ashrafi)

Received 15 June 2019; Accepted 27 November 2019

ABSTRACT

In this study, the photocatalytic degradation of 2,4,6-trichlorophenol (2,4,6-TCP) was evaluated under UV radiation by Fe-doped titanium dioxide (Fe-doped TiO₂) nanoparticles (NPs) which were synthesized by a sol-gel method. Diffuse reflectance spectroscopy (DRS), X-ray diffraction (XRD), and scanning electron microscopy (SEM) were applied to identify the synthesized nanoparticles. According to the SEM image, the synthesized nanoparticles had fine and irregular shapes with relatively smooth surfaces, as well as XRD spectrum showed that the crystalline size of Fe-doped TiO₂ NPs was 10.42 nm, furthermore, according to the DRS analysis, the bandgap energy of Fe-doped TiO₂ NPs was determined about 2.9 eV. The effects of operating parameters, including initial 2,4,6-TCP concentration, pH, contact time and Fe-doped TiO₂ NPs dosage on 2,4,6-TCP degradation were studied and optimized based on the response surface methodology with Box–Behnken method. The analysis of 2,4,6-TCP degradation showed that under optimum conditions, the removal efficiency reached 95.9% which is consistent with the model prediction. The optimum degradation conditions were as follows: pH, 3.29; initial 2,4,6-TCP concentration, 50.5 mg L⁻¹; Fe-doped TiO₂ NPs dosage, 0.59 g L⁻¹; and contact time, 55.7 min. The present results showed that Fe-doped TiO₂ NPs have great potential for removing 2,4,6-TCP from aqueous solutions.

Keywords: 2,4,6-TCP; Photocatalytic degradation; Fe-doped TiO₂; Response surface methodology

1. Introduction

Phenolic compounds are one of the most important environmental pollutants produced by artificial and natural processes. The major sources of these compounds include wastewater from different industries (e.g., paper and pulp, paint and pigment, and pharmaceutical industries) and

burning of municipal waste including pesticides, disinfectants, wood preservatives, leather, and fiber [1–3].

Trichlorophenols (TCPs), especially 2,4,6-trichlorophenol (2,4,6-TCP) are the best known phenolic compounds due to their high stability and solubility in water and wastewater. These compounds are associated with several health problems such as carcinogenesis and mutagenicity; therefore,

* Corresponding author.

the removal of these pollutants from water and wastewater is very important. TCPs can be entered into the food chain and the human body through aquatic microorganisms, animals, and plants [4,5]. On the other hand, their adverse effects on the cardiovascular, gastrointestinal, respiratory, and nervous systems have been reported in the literature [6,7]. According to the Environmental Protection Agency (EPA), 2,4,6-TCP is a major environmental pollutant. These compounds (2,4,6-TCP) cannot be effectively removed in conventional wastewater treatment systems (including biological methods) because of its toxicity for various microorganisms, in other words, 2,4,6-TCP is one of the most toxic and resistant chlorophenols against biological degradation.

Several methods, including chemical oxidation, solvent adsorption, distillation, membrane processes, electrochemical adsorption, ion exchange, and reverse osmosis, have been proposed for the removal of phenolic compounds. These methods have multiple disadvantages, such as high cost, low efficiency, long processing time, and production of secondary pollution [7–13]. To overcome these issues, more suitable methods have been proposed, such as advanced photocatalytic oxidation method. Generally, in photocatalytic degradation, pollutants are degraded under ultraviolet (UV) radiation in the presence of nanoparticles (NPs), such as titanium dioxide (TiO₂) [8,9,14].

With regard to the high optical activity, non-toxicity, cost-effectiveness, chemical stability, and electron characteristics of TiO₂, it is considered as the most common semiconductor photo-catalyst for removing of pollutants from water and wastewater [12,14,15]. So far, various approaches have been proposed to increase of photo-catalyst activity of TiO₂, including doping with metallic and non-metallic ions. Ferric ion (Fe⁺³), due to its semi-filled electron arrangement with an ionic radius close to Ti⁴⁺, can be easily substituted in the TiO₂ crystallite structure and improve the photo-catalyst activity under the visible light region [16].

Response surface methodology (RSM) is a mathematical and statistical method that is suitable for the optimization of chemical and industrial processes as well as for experimental designs. In statistics, RSM seeks the relation between several explanatory variables and one or more response variables. The main idea of RSM is the use of a sequence of designed experiments to achieve an optimum response [10,11,17–19].

According to the literature, different independent variables, such as the initial concentration of 2,4,6-TCP, pH, contact time, and Fe-doped TiO₂ NPs dosage, affect on TCP removal in the photo-catalytic process. The present study aimed to determine the effects of these variables on 2,4,6-TCP degradation, examining the relationship between these experimental variables, and optimizing the experimental conditions based on RSM.

2. Materials and methods

The required materials were purchased from reputable companies. Sigma-Aldrich provided titanium tetra-isopropoxide (TTIP; purity, 97%) and 2,4,6-TCP. Also, Merck supplied ethanol 99% (C₂H₆O) and nitric acid (HNO₃). Standard solutions were prepared using deionized water.

The Fe-doped TiO₂ NPs catalyst was synthesized by a sol-gel method, with TTIP as the starting material. In the

synthesis process, Fe(NO₃)₂ (0.25 g) and deionized water (6 mL) was dissolved in ethanol (30 mL) and were shaken for 15 min (solution No. 1). In other erlen, TTIP (9 mL) was added to the rest of ethanol (60 mL) (solution No. 2) and agitated for 30 min. Solution No. 1 was added dropwise into the solution No. 2, the produced sol was obtained and kept at the room temperature for gel formation. To remove alcohol, the gel was placed in an oven for 24 h at 80°C. Next, deionized water was used several times for washing of obtained white powder; finally, it was calcinated at 500°C for 1 h. For characterizing the synthesized Fe-doped TiO₂ NPs, diffuse reflectance spectroscopy (DRS), X-ray diffraction (XRD), and scanning electron microscopy (SEM) were performed.

Before starting of the photo-catalytic process, the impact of adsorption/desorption reaction was investigated on process efficiency. For adsorption/desorption, the samples were put in the darkness condition for 30 min and after that, the samples were placed under irradiation in the photocatalytic reactor. To investigate the potential of synthesized NPs as a catalyst in the photocatalytic reactor and as well as to evaluate the effects of independent variables on the removal efficiency of 2,4,6-TCP, the photo-catalytic process was performed in a Plexiglas batch reactor via UV irradiation. The 2,4,6-TCP solutions were prepared at 50, 100, and 150 mg L⁻¹ for the photo-catalytic process; pH was also adjusted by HNO₃ and NaOH 0.1 N in the range of 3, 7, and 11. In addition, different dosages of Fe-doped TiO₂ NPs (0.2, 0.4, and 0.6 g L⁻¹) were added to the solution and irradiated under a UV lamp (15 W) for 30, 60, and 90 min. Moreover, gas chromatography (GC) was used to determine the concentration of residual 2,4,6-TCP to determine the removal efficiency of 2,4,6-TCP.

Dispersive liquid–liquid micro-extraction (DLLME) technique was used to extract organic-phase 2,4,6-TCP from the aqueous solution. After irradiation of solution within predefined times, a certain amount of solution (5 mL of sodium carbonate 5%; pH, 8–11) was added into a Falcon centrifuge tube (10 mL). A mixture of propanol (1 mL) as the solvent and dichloromethane (2 mL) as the extraction solvent was rapidly added into the aqueous sample. After 10 min of shaking, the sample was centrifuged for 5 min at 4,000 rpm. Next, 1 μL of the settled organic phase was injected into the GC device (Agilent, USA).

In this study, the experiment design was plotted in Design-Expert Software and Box–Behnken Design RSM was applied to investigate the effects of pH (A), catalyst dose (B), initial concentration (C) and contact time (D) on the 2,4,6-TCP removal in photo-catalyst process. Based on the random order indicated by RSM, a total of 29 runs were performed (Table 1). The use of RSM provides a mathematical relationship between factors and the experimental results that can be fitted to a second-order polynomial model as Eqs. (1).

$$\text{Response} = \beta_0 + \beta_1 A + \beta_2 B + \beta_3 C + \beta_4 D + \beta_5 AB + \beta_6 AC + \beta_7 AD + \beta_8 BC + \beta_9 BD + \beta_{10} CD + \beta_{11} A^2 + \beta_{12} B^2 + \beta_{13} C^2 + \beta_{14} D^2 \quad (1)$$

In this equation, $\beta_1, \beta_2, \beta_3, \dots, \beta_{20}$ are coefficients of the regression equation. In the current study, to determine the quality of the proposed model, R^2 and R^2_{Adjusted} , as well

Table 1
RSM values based on the Box–Behnken design

Run order	Blocks	pH	Fe–TiO ₂	2,4,6-TCP concentration (mg L ⁻¹)	Contact time (minutes)	Removal %
9	1	3	0.4	100	30	74.00
17	1	3	0.4	100	90	81.00
19	1	3	0.4	150	60	71.00
24	1	3	0.6	100	60	93.00
25	1	3	0.4	50	60	85.00
27	1	3	0.2	100	60	62.00
1	1	7	0.2	100	90	31.00
2	1	7	0.6	100	90	56.00
3	1	7	0.4	100	60	43.04
5	1	7	0.4	100	60	42.60
6	1	7	0.4	100	60	40.87
8	1	7	0.2	50	60	33.40
10	1	7	0.2	100	30	29.11
11	1	7	0.4	100	60	41.76
12	1	7	0.2	150	60	28.23
14	1	7	0.6	100	30	52.00
15	1	7	0.6	50	60	58.00
16	1	7	0.4	150	30	35.00
18	1	7	0.6	150	60	49.00
20	1	7	0.4	50	30	45.00
21	1	7	0.4	100	60	42.00
23	1	7	0.4	50	90	48.00
26	1	7	0.4	150	90	39.00
4	1	11	0.4	100	90	24.00
7	1	11	0.4	100	30	22.00
13	1	11	0.4	150	60	19.00
22	1	11	0.6	100	60	28.12
28	1	11	0.2	100	60	13.00
29	1	11	0.4	50	60	26.34

as the plot of normal distribution of the residuals, were obtained. Analysis of variance (ANOVA) was used as the method of statistical analysis of responses and p -value < 0.05 or lack of fit > 0.05 was considered as significant of statistical model, and also the corresponding plots were designed to better understand the effect of the variable.

3. Results and discussion

3.1. Characterization of synthesized NPs

3.1.1. SEM analysis

SEM image showed that the synthesized NPs have fine and irregular shapes with relatively smooth surfaces. The primary particles tend to agglomerate into larger particles. NPs agglomeration might be related to the association between Fe doping and new crystal lattice defects. According to the SEM analysis (Fig. 1), the size of Fe-doped TiO₂ NPs was 14–25 nm.

3.1.2. XRD analysis

To confirm the crystalline characteristics and structure, XRD analysis was performed on the synthesized doped and un-doped NPs. The XRD patterns corresponding to the synthesized NPs were in the range of $2\theta = 10^\circ$ – 80° , with Cu Ka radiation (0.15406 nm) as the X-ray source (100 mA, 40 kV). The XRD patterns of doped and un-doped NPs showed similar intense diffraction peaks at $2\theta = 25.88^\circ$, 37.75° , 48.28° , 54.55° , and 56.28° , respectively (Fig. 2). The peaks of Fe-doped TiO₂ NPs showed broadening in comparison with the un-doped NPs, which might be attributed to the reduced particle size, causing a reduction in crystallite size and an increase in crystal defects.

Furthermore, comparison of Fe-doped with un-doped NPs showed no detectable peak for the dopant; this might be related to the transfer of low quantities of Fe ions (for preparation of Fe-doped NPs) into the interstitial or substitutional site of TiO₂, considering the similarities in the ionic radius of Fe³⁺ and Ti⁴⁺ ions. Based on the Debye–Scherrer's

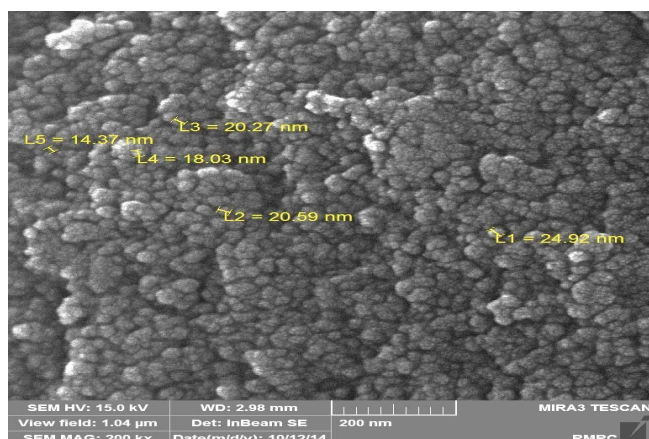


Fig. 1. SEM image of the structure of doped TiO₂ NPs.

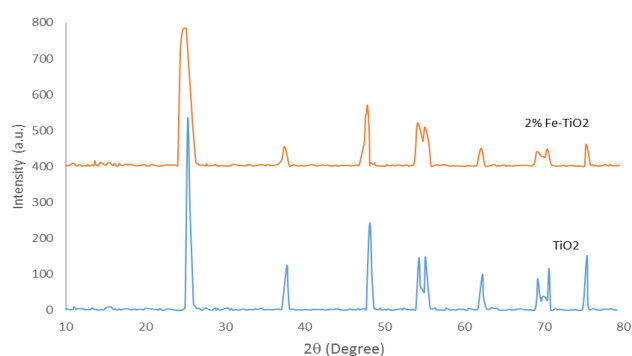


Fig. 2. XRD analysis of doped TiO₂ NPs.

formula, the average crystallite size was measured in NPs with respect to the FWHM of the diffraction pattern. The crystallite size of Fe-doped NPs was reduced compared to the un-doped NPs (Fe-doped TiO₂, $D = 10.42$ nm; TiO₂, $D = 21$ nm). The crystallite size reduction in Fe-doped TiO₂ could be related to iron incorporation into the TiO₂ network.

3.1.3. DRS analysis

UV-VIS DRS (300–700 nm) was performed to describe the optical absorption of TiO₂ and Fe-doped TiO₂ NPs. Light absorption in UV wavelengths is usually linked to electron transfer from the valence to the conduction band. According to Fig. 3a, the light absorption edge of un-doped and doped NPs was nearly 400 and 410 nm, respectively. The redshift observed in the light absorption edge may be attributed to the narrowing of the TiO₂ bandgap. The Kubelka–Munk equation was also calculated to determine the bandgap energy of synthesized NPs.

The analysis of band gap energies indicated that by increasing of Fe doping from 0 to 2 weight percent, the band gap energy is reduced from 3.10 to 2.90 eV (Fig. 3b), considering the charge transition; however, the obtained band gap energy is lower than that of commercial TiO₂ (P25 TiO₂; 3.2 eV). The reduction of band gap indicates that Fe-doped TiO₂ NPs could be activated at higher UV and Vis wavelengths. Doping with Fe ions also leads to the formation of

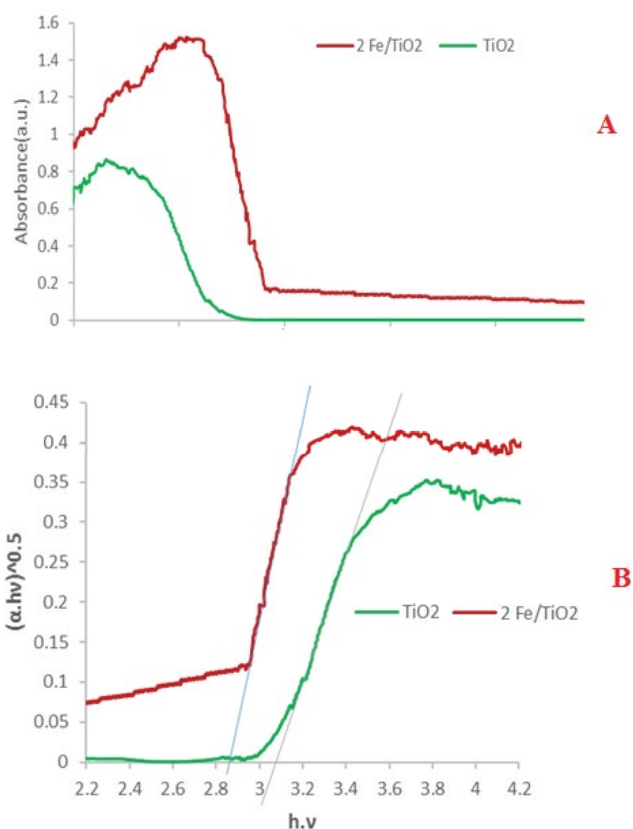


Fig. 3. DRS of TiO₂ and doped TiO₂ NPs (a) and reduction of energy gap after Fe doping (b).

empty oxygen spaces in the crystal lattice, which promotes further reactions. Comparison of un-doped TiO₂ NPs with commercial TiO₂ (energy gap, 3.2 eV) indicates that the synthesized NPs have a smaller energy gap, which might vary during synthesis, based on the sol-gel method.

3.2. RSM of experimental data

The results of experiments, according to the Box–Behnken design, are summarized in Table 1. This table shows the experimental design matrix of the Box–Behnken model and the actual of 2,4,6-TCP removal. The adequacy and significance of the model were examined using ANOVA test. The results of ANOVA and regression analysis are presented in Table 2. F -value and P -value for the linear model were 2,168.52 and <0.05 , respectively. As shown in Table 2, parameters with $P < 0.05$ had significant effects on the removal efficiency. According to this table, the lack-of-fit parameter is insignificant (0.431); therefore, the selected model had no defects in describing the data. Therefore, the linear model to predict the removal percentage of 2,4,6-TCP from aqueous solution was achieved. This model has been shown in Eq. (2) with four factors.

$$\begin{aligned} \text{Removal (\%)} = & 83.34 - 12.045 \text{ pH} + 104.0 \text{ Fe-TiO}_2 - 0.1344 \\ & \text{TCP} + 0.0737 \text{ time} + 0.4910 \text{ pH}^2 - 4.963 \text{ pH} \times \text{Fe-TiO}_2 + \\ & 0.00832 \text{ pH} \times \text{TCP} - 0.01042 \text{ pH} \times \text{time} \end{aligned} \quad (2)$$

Table 2
ANOVA test of linear RSM model for fluoride removal

Source	DF	Adjusted SS	Adjusted MS	F-value	P-value
Model	14	11,699.6	835.69	648.53	0.000
Linear	4	11,177.2	2,794.30	2,168.52	0.000
pH	1	9,270.7	9,270.74	7,194.57	0.000
Fe-doped TiO ₂	1	1,618.9	1,618.90	1,256.35	0.000
2,4,6-TCP Con.	1	247.6	247.61	192.16	0.000
Time	1	39.9	39.93	30.99	0.000
Square	4	437.0	109.25	84.79	0.000
pH × pH	1	400.3	400.27	310.63	0.000
Fe-TiO ₂ Con. × Fe-TiO ₂ Con.	1	0.8	0.77	0.60	0.452
2,4,6-TCP Con. × 2,4,6-TCP Con.	1	0.2	0.19	0.14	0.710
Time × time	1	0.0	0.02	0.02	0.892
Two-way interaction	6	85.4	14.24	11.05	0.000
pH × Fe-doped TiO ₂	1	63.0	63.04	48.93	0.000
pH × 2,4,6-TCP Con.	1	11.1	11.09	8.61	0.011
pH × time	1	6.2	6.25	4.85	0.045
Fe-doped TiO ₂ × 2,4,6-TCP Con.	1	3.7	3.67	2.85	0.114
Fe-doped TiO ₂ × Time	1	1.1	1.11	0.86	0.368
2,4,6-TCP Con. × Time	1	0.2	0.25	0.19	0.666
Error	14	18.0	1.29		
Lack-of-fit parameter	10	15.3	1.53	2.21	0.231
Pure error	4	2.8	0.69		
Total	28	11,717.6			

Fig. 4 represents the standardized effects plot of each factor and its association with removal efficiency (%). The normal probability plot has two right and left regions, representing the positive and negative coefficients, respectively (Fig. 4). Factors presented as square are regarded as significant. As can be seen, the predicted values showed a good correlation with the actual values.

3.3. Effect of Fe-doped TiO₂ NPs

Figs. 5, 6a and d indicate the effect of Fe-doped TiO₂ NPs on 2,4,6-TCP removal. The increase in Fe-doped TiO₂ NPs dosage improved the removal efficiency of 2,4,6-TCP due to an increase in the adsorption sites available on the NPs catalyst, which subsequently increases the possibility of further collisions between 2,4,6-TCP and TiO₂ NPs, as well as oxidation-reduction reactions. However, at lower dosages, the available sites which are necessary to the removal of pollutants over time are decreased and consequently, the removal efficiency is reduced [20]. In the study conducted by Liu et al. [9]; the effects of Fe/TiO₂ dosage were investigated on the photocatalytic degradation of 2,4-dichlorophenol and they reported similar results. Moreover, in another study conducted by Yang et al. [21]; the effects of Fe₃O₄/g-C₃N₄ were investigated for 2,4,6-TCP photo-degradation and its results showed that the removal percentage is increased as the catalyst level is increased.

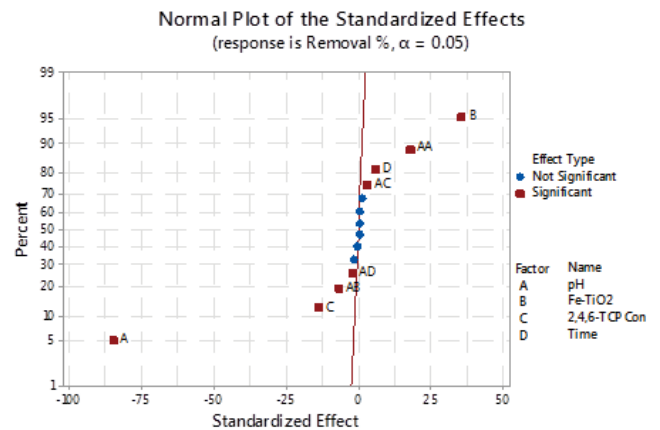


Fig. 4. Predicted vs. actual rates of 2,4,6-TCP removal efficiency.

3.4. Effect of pH

Figs. 5 and 6a–c represents the effect of pH on removal efficiency. It is known that the pH of the solution is a significant parameter in chemical reactions in water and wastewater treatment processes. According to the many published articles, it is also an important factor, affecting the photocatalytic oxidation process. In the acidic pH range, a high level of pollutants can be eliminated. Fe-doped TiO₂ particles

have a positive charge in acidic pH, which can easily adsorb ionized chlorophenol with a negative charge; therefore, major traction occurs with pollutant ions. By increasing of pH and subsequently increase of negative NPs, the adsorption efficiency decreases due to a repulsive force.

Chlorophenols are known as proton donors. Therefore, they become anionic when the pH solution exceeds the pKa of chlorophenol (pKa of chlorophenol is nearly 9.52). At the high pH of the solution, the attraction force is decreased between Fe-TiO₂-negative groups and phenoxide ions as a result of repulsive force. Therefore, in the present study, the percentage of pollutant removal had an inverse relationship with pH, and the removal percentage was decreased at high and alkaline pH. [21]. Zhang et al. also found similar results in their study [22].

Additionally, Kamali et al. [23] evaluated the nano-photocatalytic effects of UV/Fe-doped TiO₂ on the removal of cis-chlordane from water. Consistent with the present study, they showed that by reducing pH, the removal efficiency is increased. The effect of pH in this study is consistent with many other previous studies. Based on the findings, at intermediate levels of other variables, the removal efficiency was increased by decreasing pH from 11 to 3. Regarding the

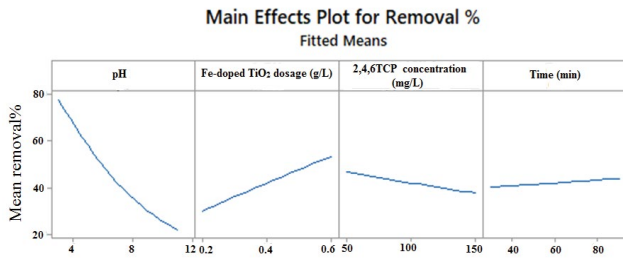


Fig. 5. Effect of pH, Fe-doped TiO₂ concentration, contact time, and 2,4,6-TCP concentration on removal efficiency.

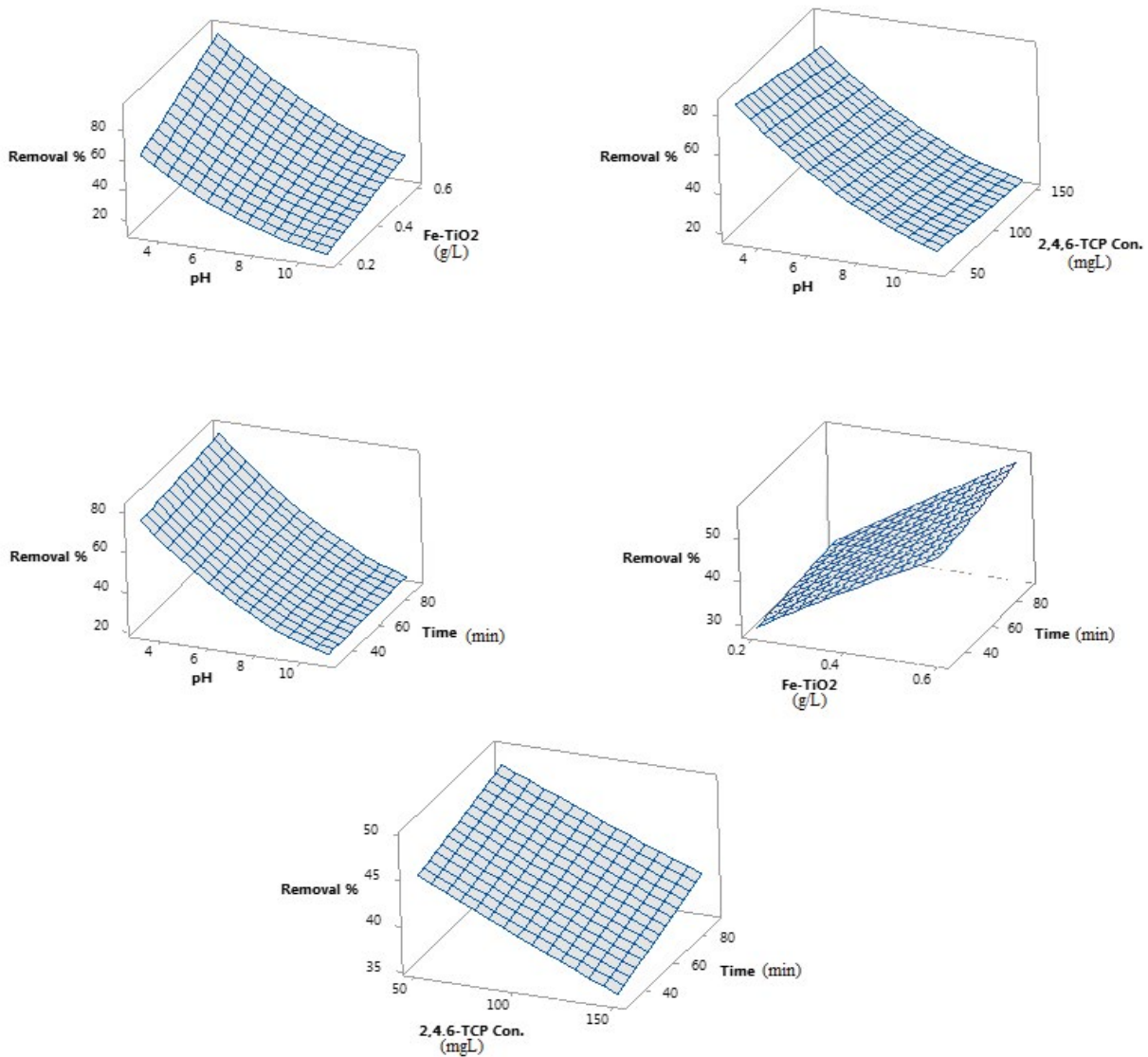


Fig. 6. Contour plots of removal efficiency vs. contact time and 2,4,6-TCP concentration; contact time and Fe-doped TiO₂ concentration; pH and contact time; pH and 2,4,6-TCP concentration; pH and Fe-TiO₂ concentration.

anionic 2,4,6-TCP behavior, it can be stated that pH reduction (an increase of positive charge on the catalyst surface), resulting in the strengthening of electrostatic gravity forces, is more suitable for increasing contact with 2,4,6-TCP on the catalyst.

3.5. Effect of contact time

According to Figs. 5 and 6c–e, the removal efficiency of 2,4,6-TCP was decreased at all studied concentrations with an increase in contact time from 30 to 90 min. Yuan et al. [24] also found similar results in their study. In the present study, the removal efficiency was improved by increasing the contact time, while photocatalytic removal occurred more rapidly within early time. Over time, due to the reduction of free catalyst sites and pollutant concentrations, the removal rate was reduced at a later time. Various studies have shown that in the photocatalytic process, removal of pollutants follows first-order kinetics. Evidence shows that the removal of pollutants in early reactions is much faster than later reactions. Also, statistical analysis showed a significant relationship between contact time and efficiency of 2,4,6-TCP removal by NPs.

3.6. Effect of initial 2,4,6-TCP concentration

The effect of initial TCP concentration on removal efficiency is shown in Figs. 5, 6b and e. The removal efficiency was inversely related to the concentration of 2,4,6-TCP; this can be attributed to the association between the increase in the initial concentration of pollutants and the increased collision of 2,4,6-TCP molecules with the catalyst surface. Although the increased 2,4,6-TCP concentration and subsequently the increased force of mass transfer stimulates the adsorption capacity on the catalyst, the removal efficiency of 2,4,6-TCP was reduced considering the saturation of active sites on the surface of the catalyst. Overall, the amount of 2,4,6-TCP degradation can be controlled by limiting the number of available adsorption sites from the photocatalyst. Under similar conditions for all samples, the produced amount of hydroxyl radicals at each initial 2,4,6-TCP concentration is equal; therefore, the percentage of 2,4,6-TCP removal in samples with lower concentrations is expected to be higher [8,9].

In this regard, Kamali et al. [23] examined the nano-photocatalytic effects of UV/Fe-doped TiO₂ on the removal of cis-chlordane in water solution. The removal efficiency of pollutants was reduced by decreasing its concentration. Also, in a study by Yang et al., different 2,4,6-TCP concentrations (10–200 mg L⁻¹) were examined to describe the synthesis of Fe₃O₄/g-C₃N₄ nanocomposites and their application in 2,4,6-TCP photodegradation. The degradation percentage was decreased as the initial 2,4,6-TCP concentration was increased; the highest removal of 2,4,6-TCP was reported at 50 mg L⁻¹ [21].

In the degradation of phenolic compounds at high concentrations, polymeric compounds such as phenols which are water-insoluble and likely to bind to the catalyst surface. This can be considered for the effectiveness of photocatalytic reactions at higher concentrations of TCP. Sobczykński et al. [25] presented similar results and explained the formation

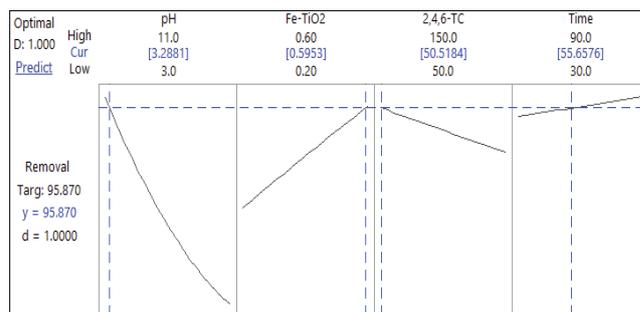


Fig. 7. Removal efficiency under optimal conditions.

of insoluble polymer compounds. Xu et al. [26] also found similar results in their study.

3.7. Optimization and confirmation

In the optimization process, the purpose is to find a combination of levels of variables that maximally eliminate 2,4,6-TCP. The RSM selects and predicts the best operating mode between the ranges of utilized variables [27–29]. The optimum conditions for 2,4,6-TCP removal and optimum removal efficiencies are presented in Fig. 7. The predicted optimum pH, Fe-TiO₂ dosage, TCP concentration, and contact time were 3.29, 0.59 g L⁻¹, 50.5 mg L⁻¹, and 55.7 min, respectively (Fig. 7).

4. Conclusion

In this research, we studied the modeling of 2,4,6-TCP photo-catalytic removal in aqueous solutions using synthesized Fe-doped TiO₂ NPs based on RSM. The SEM analysis showed that Fe-doped TiO₂ NPs have a spherical structure, with an average size of 19.63 nm. The RSM method using Design-Expert software was used to experimental design and analysis of data as well as modeling of 2,4,6-TCP removal in the photocatalytic reaction. The results revealed that the best model for predicting 2,4,6-TCP removal is linear model. The optimum conditions for maximum 2,4,6-TCP removal (95.9%) were as follows: initial 2,4,6-TCP concentration, 50.5 mg L⁻¹; catalyst dosage, 0.59 g L⁻¹; pH, 3.29; and contact time, 55.7 min. These results show that the Fe-doped TiO₂ NPs nanoparticles were a suitable catalyst for 2,4,6-TCP degradation in the photo-catalytic treatment systems.

Acknowledgments

This paper was a part of the research that has been registered in the Ethics Committee under ID no: IR. ZAUMS. REC.1396.141 and supported financially by a grant (No. 8257) from the Zahedan University of Medical Sciences, Zahedan, Iran.

References

- [1] T. Anirudhan, M. Ramachandran, Removal of 2,4,6-trichlorophenol from water and petroleum refinery industry effluents by surfactant-modified bentonite, *J. Water Process Eng.*, 1 (2014) 46–53.
- [2] J. Fan, J. Zhang, C. Zhang, L. Ren, Q. Shi, Adsorption of 2,4,6-trichlorophenol from aqueous solution onto activated

- carbon derived from looestrife, *Desalination*, 267 (2011) 139–146.
- [3] Z. Zango, Z.N. Garba, N.A. Bakar, W. Tan, M.A. Bakar, Adsorption studies of Cu²⁺-Hal nanocomposites for the removal of 2,4,6-trichlorophenol, *Appl. Clay Sci.*, 132 (2016) 68–78.
- [4] Z.N. Garba, A.A. Rahim, Optimization of activated carbon preparation conditions from *Prosopis africana* seed hulls for the removal of 2,4,6-Trichlorophenol from aqueous solution, *Desal. Wat. Treat.*, 56 (2015) 2879–2889.
- [5] B. Hameed, I. Tan, A. Ahmad, Adsorption isotherm, kinetic modeling and mechanism of 2,4,6-trichlorophenol on coconut husk-based activated carbon, *Chem. Eng. J.*, 144 (2008) 235–244.
- [6] B. Gao, L. Liu, J. Liu, F. Yang, Photocatalytic degradation of 2,4,6-tribromophenol over Fe-doped ZnIn₂S₄: stable activity and enhanced debromination, *Appl. Catal., B*, 129 (2013) 89–97.
- [7] I. Tan, A. Ahmad, B. Hameed, Adsorption isotherms, kinetics, thermodynamics and desorption studies of 2,4,6-trichlorophenol on oil palm empty fruit bunch-based activated carbon, *J. Hazard. Mater.*, 164 (2009) 473–482.
- [8] H. Ji, F. Chang, X. Hu, W. Qin, J. Shen, Photocatalytic degradation of 2,4,6-trichlorophenol over g-C₃N₄ under visible light irradiation, *Chem. Eng. J.*, 218 (2013) 183–190.
- [9] L. Liu, F. Chen, F. Yang, Y. Chen, J. Crittenden, Photocatalytic degradation of 2,4-dichlorophenol using nanoscale Fe/TiO₂, *Chem. Eng. J.*, 181 (2012) 189–195.
- [10] E. Bazrafshan, T.J. Al-Musawi, M.F. Silva, A.H. Panahi, M. Havangi, F.K. Mostafapur, Photocatalytic degradation of catechol using ZnO nanoparticles as catalyst: optimizing the experimental parameters using the Box–Behnken statistical methodology and kinetic studies, *Microchem. J.*, 147 (2019) 643–653.
- [11] T.J. Al-Musawi, H. Kamani, E. Bazrafshan, A.H. Panahi, M.F. Silva, G. Abi, Optimization the effects of physicochemical parameters on the degradation of cephalixin in sono-fenton reactor by using Box–Behnken response surface methodology, *Catal. Lett.*, 149 (2019) 1186–1196.
- [12] H. Kamani, S. Nasser, M. Khoobi, R.N. Nodehi, A.H. Mahvi, Sonocatalytic degradation of humic acid by N-doped TiO₂ nano-particle in aqueous solution, *J. Environ. Health Sci. Eng.*, 14 (2016) 3.
- [13] E. Bazrafshan, M. Sobhanikia, F. Mostafapour, H. Kamani, D. Balarak, Chromium biosorption from aqueous environments by mucilaginous seeds of *Cydonia oblonga*: kinetic and thermodynamic studies, *Global Nest J.*, 19 (2017) 269–277.
- [14] M.M. Ba-Abbad, A.A.H. Kadhum, A.B. Mohamad, M.S. Takriff, K. Sopian, Synthesis and catalytic activity of TiO₂ nanoparticles for photochemical oxidation of concentrated chlorophenols under direct solar radiation, *Int. J. Electrochem. Sci.*, 7 (2012) 4871–4888.
- [15] H. Kamani, E. Bazrafshan, S.D. Ashrafi, F. Sancholi, Efficiency of sono-nano-catalytic process of TiO₂ nano-particle in removal of erythromycin and metronidazole from aqueous solution, *J. Mazandaran Univ. Med. Sci.*, 27 (2017) 140–154.
- [16] M.M. Ba-Abbad, A.A.H. Kadhum, A.B. Mohamad, M.S. Takriff, K. Sopian, Visible light photocatalytic activity of Fe³⁺-doped ZnO nanoparticle prepared via sol–gel technique, *Chemosphere*, 91 (2013) 1604–1611.
- [17] M. Galedari, M.M. Ghazi, S.R. Mirmasoomi, Photocatalytic process for the tetracycline removal under visible light: presenting a degradation model and optimization using response surface methodology (RSM), *Chem. Eng. Res. Des.*, 145 (2019) 323–333.
- [18] S. Mortazavian, A. Saber, D.E. James, Optimization of photocatalytic degradation of Acid Blue 113 and Acid Red 88 textile dyes in a UV-C/TiO₂ suspension system: application of response surface methodology (RSM), *Catalysts*, 9 (2019) 360.
- [19] P. Chawla, S.K. Sharma, A.P. Toor, Optimization and modeling of UV-TiO₂ mediated photocatalytic degradation of golden yellow dye through response surface methodology, *Chem. Eng. Commun.*, 206 (2019) 1123–1138.
- [20] K. Nadafi, N. Rastkari, R. Nabizadeh, M. Gholami, M. Sarkhosh, Performance of modified natural zeolite for removal of 2,4,6-trichlorophenol from aqueous solutions, *Toloo-e-Behdasht*, 12 (2014).
- [21] J. Yang, H. Chen, J. Gao, T. Yan, F. Zhou, S. Cui, W. Bi, Synthesis of Fe₃O₄/g-C₃N₄ nanocomposites and their application in the photodegradation of 2,4,6-trichlorophenol under visible light, *Mater. Lett.*, 164 (2016) 183–189.
- [22] C.-L. Zhang, S.-J. Cui, Y. Wang, Adsorption removal of pefloxacin from water by halloysite nanotubes, *J. Ind. Eng. Chem.*, 23 (2015) 12–15.
- [23] M. Kamali, K. Dindarlo, O. Rahmaniyan, V. Alipoor, Nanophotocatalytic activity of UV/Fe-doped TiO₂ for removal of cis-chlordane from water, *J. Prevent. Med.*, 3 (2017) 52–43.
- [24] S. Yuan, X. Mao, A.N. Alshawabkeh, Efficient degradation of TCE in groundwater using Pd and electro-generated H₂ and O₂: a shift in pathway from hydrodechlorination to oxidation in the presence of ferrous ions, *Environ. Sci. Technol.*, 46 (2012) 3398–3405.
- [25] A. Sobczynski, L. Duczmal, W. Zmudzinski, Phenol destruction by photocatalysis on TiO₂: an attempt to solve the reaction mechanism, *J. Mol. Catal. A: Chem.*, 213 (2004) 225–230.
- [26] L. Xu, J. Wang, Degradation of 2,4,6-trichlorophenol using magnetic nanoscaled Fe₃O₄/CeO₂ composite as a heterogeneous Fenton-like catalyst, *Sep. Purif. Technol.*, 149 (2015) 255–264.
- [27] S.-N. Nam, H. Cho, J. Han, N. Her, J. Yoon, Photocatalytic degradation of acesulfame K: optimization using the Box–Behnken design (BBD), *Process Saf. Environ. Prot.*, 113 (2018) 10–21.
- [28] P. Singh, A. Dhir, V.K. Sangal, Optimization of photocatalytic process parameters for the degradation of acrylonitrile using Box–Behnken design, *Desal. Wat. Treat.*, 55 (2015) 1501–1508.
- [29] S. Sohrabi, F. Akhlaghian, Modeling and optimization of phenol degradation over copper-doped titanium dioxide photocatalyst using response surface methodology, *Process Saf. Environ. Prot.*, 99 (2016) 120–128.